

Seismic Protection of Structures Using Novel Negative Stiffness Device



A. A. Sarlis, M. C. Constantinou & A. M. Reinhorn

Dept. of Civil and Envi. Engineering, University at Buffalo, Buffalo, NY-14260, USA.

D. T. R. Pasala & S. Nagarajaiah

Dept. of Civil and Environmental Engineering, Rice University, Houston, TX-77005, USA.

D. Taylor

Taylor Devices Inc., North Tonawanda, NY-14120 U.S.A.

SUMMARY:

Structural weakening and addition of damping is an approach previously proposed for the reduction of seismic forces and drifts in the retrofit of structures. It is also used in the design of new buildings with damping systems. While this approach is efficient, it does not significantly reduce and may even amplify inelastic excursions and permanent deformations of the structural system during a seismic event. This paper describes a negative stiffness device (NSD) that can emulate weakening of the structural system without inelastic excursions and permanent deformations. The NSD simulates yielding by engaging at a prescribed displacement and by applying a force at its installation level that opposes the structural restoring force. This paper reports the development and operation of the NSD and presents analytical and computational tools that describe the behavior of the device.

Keywords: Negative Stiffness, Nonlinear Elastic Device, Adaptive Negative Stiffness Device (NSD)

1. INTRODUCTION

Current practice for designing structures against seismic actions relies on ductile behavior and allows the development of significant inelastic deformations in strong earthquakes so that reduction of inertia forces is achieved. At best, this approach ensures life safety in the design earthquake event and collapse prevention in the maximum earthquake event. Large drifts, permanent deformations and loss of functionality of the structure are common observations of performance after strong seismic events. Reinhorn et al (2005) and Viti et al (2006) introduced the concept of weakening (reducing strength and implicitly stiffness) and introduction of supplemental viscous damping to simultaneously reduce structural accelerations and inter-story drifts in the retrofit of structures. Moreover, the approach described in ASCE 7, Chapter 18 (American, 2010) for the design of structures with damping systems is based on the concept of reduced strength and stiffness and addition of damping to achieve the same objective for new construction (Ramirez et al, 2001). Specifically, new buildings designed with viscous damping systems per minimum criteria of the ASCE 7 Standard, Chapter 18 have strength and stiffness approximately half of that of a comparable building without the damping system that also meets the drift criteria (Ramirez et al, 2001). However, the approach does not reduce inelastic action or improve the performance of the structural system unless enhanced viscous damping is used to achieve a higher performance level (Ramirez et al, 2001; Pavlou et al, 2006). An alternative approach is to “simulate yielding” by introducing true negative stiffness at prescribed displacements leading to the concept of “apparent weakening” (see Nagarajaiah et al, 2010 and Pasala et al, 2012).

True negative stiffness means that a force is introduced to assist motion, not to oppose it. The device developed in this work uses a passive mechanical system to generate the negative stiffness and it does not need any external power supply. The concept of negative stiffness was first introduced in the pioneering publication of Molyneaux (1957) in several proposals for vibration isolation systems. This original idea recently became reality in the development of highly effective vibration isolation systems (e.g., see US patent 6676101BB2; Platus, 2004). Thus far the application of negative stiffness devices has been limited to vibration isolation of small, highly sensitive equipment and of seats in automobiles

(Lee et al (2007)). The reason that this technology has been restricted to small mass applications is due to the requirement for large forces to develop the necessary negative stiffness. These preload forces are typically of the order of the weight of the isolated structure. The application of negative-stiffness concept to massive structures, like buildings and bridges, requires modification of the existing mechanisms to reduce the demand for preload force and to “package” the negative stiffness device in a system that does not impose any additional loads on the structure, other than those needed for achieving the goal of seismic protection. These requirements lead to the development of the true negative system device described in this paper (termed Negative Stiffness Device or NSD).

Note that other negative stiffness concepts have also been developed and tested for structures, but they lack the important characteristics that can be achieved using the NSD. One example is the pseudo negative stiffness system developed by Iemura et al (2009) which makes use of active or semiactive hydraulic devices to develop negative stiffness. Another example is the one described by Iemura et al (2009) in which a structure is placed on top of convex pendulum bearings. Negative stiffness is generated due to the structure’s vertical loads applied on the convex surface (as opposed to the behavior of Friction Pendulum bearings that utilize concave surfaces-see Fenz et al, 2008-and in similarity to the behavior of the uplift-restraining Friction Pendulum bearing-see Roussis et al, 2006) while elastomeric bearings placed in parallel provide positive stiffness. Their combination however generates a system of low effective stiffness that emulates the behavior of single Friction Pendulum bearings. Additional implications might arise due to the fact that the vertical loads are transferred through an unstable system which generates constant negative stiffness for all displacement amplitudes.

2. NEGATIVE STIFFNESS DEVICE (NSD) DESCRIPTION

The NSD is shown in Fig. 2.1. (photographs) and schematically in Fig. 2.2. in un-deformed and deformed configurations. The device consists of a pre-compressed spring in the center of the device and two GSAs at the bottom. The pre-compressed spring is connected with a link mechanism which transfers horizontal loads to the upper and lower part of the frame. When the device deforms in one direction, the pre-compressed spring rotates and creates a force that assists motion, thus creating the negative stiffness.



Figure 2.1. Views of Negative Stiffness Device [(a): Un-deformed NSD; (b): Deformed NSD]

Consider that point A (or the top of the device) moves to the right as shown in Fig. 2.2.(b). The lever-AB imposes a displacement on point B, which causes plate BCD to rotate about the pivot C. Due to the axial rigidity of the lever and its negligible rigid body rotation, the imposed displacement at point A and the displacement of point B are practically equal. Point D moves in the direction opposing the displacement of point A. Point E is rigidly connected to the top of the device (through the top chevron brace) and therefore has a displacement equal to that of point A. Due to the kinematics of points D and E, the pre-compressed spring rotates and its force facilitates the motion rather than opposing it. Note that the motion of point D relative to point E (extension of spring) is magnified by comparison to the motion of point A (a) by the ratio of the lever (distance DC to CB) and (b) by additional factor due to combination of movement of point E by the same amount as point A and the existence of the lever.

The spring exhibits its minimum length when the device is un-deformed. As the device deforms, the spring extends, its pre-compression force reduces, its angle of inclination increases and the negative stiffness magnitude generated by the device reduces. This is illustrated in the lateral force-displacement relation of the NSD without the GSA contribution shown in Fig. 2.3.(a). Note that this negative stiffness reduction eventually leads to positive stiffness at larger displacements. This is a desired effect, which is termed “stiffening” in this paper. Stiffening can be very important in earthquakes beyond the maximum considered earthquake where it can act as displacement restrainer.

Each of the two GSAs is bolted to the bottom of the device and is connected to the top chevron brace through simple compression contact, as shown in Fig. 2.2.(b). When point A moves to the right, point E moves by the same amount and compresses one of the GSA. The compressed GSA has the lateral force-displacement relation shown in Fig. 2.3.(b), which when added to the force-displacement relation of the NSD (Fig. 2.3.(a)) results in the relation shown in Fig. 2.3.(c). Negative stiffness is eliminated for displacements less than the apparent-yield displacement u'_y (also termed as NSD engagement displacement). The GSA can be designed to generate a positive stiffness equal to or slightly larger than the negative stiffness at zero displacement so that effectively the total stiffness generated by the NSD for displacements less than u'_y is approximately zero or slightly larger than zero as shown in Fig. 2.3.(c). Note that the large compressive force in the pre-loaded spring is in equilibrium with compressive forces in the double-hinged columns of the assembly (see Fig. 2.1. and Fig. 2.2.).

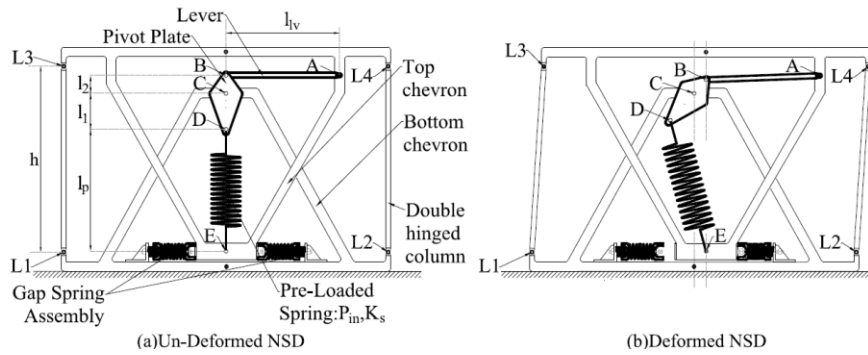


Figure 2.2. Schematics of Negative Stiffness Device

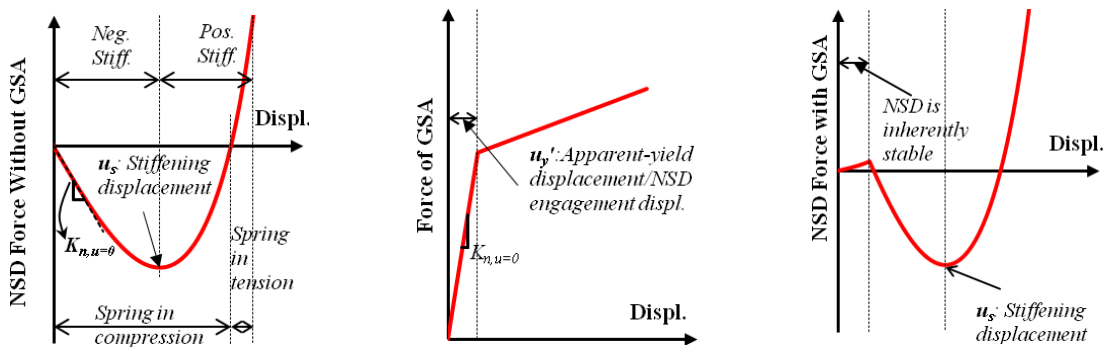


Figure 2.3. Ideal Force-displacement Relations of Components of Negative Stiffness Device [(a): NSD w/out GSA; (b): GSA; (c): NSD w/ GSA]

3. ANALYTICAL MODEL OF NEGATIVE STIFFNESS DEVICE

First consider the device without the GSA (Gap Spring Assembly Mechanism). The deformed shape of the center link mechanism made of the spring and the pivot plate and the forces acting on a free body diagram of the device are shown in Fig. 3.1. The lateral displacement of the top of the device with respect to the bottom is u and is considered equal to the displacements of points B and E

(assuming rigid members and negligible rotation of the lever). In Fig. 3.1., l_2 is the length of the pivot plate from point-C to point-B, l_1 is the length from point-C to point-D, θ_s is the inclination angle of the spring, θ_p is the angle of the pivot plate with respect to vertical. From geometry and considering that point C is fixed (connected to the bottom of the device), the displacements and angles θ_s and θ_p are given by:

$$u_B = u_E = -u_D l_2/l_1 = u; \theta_s = \arcsin\left[u(1+l_1/l_2)/l_s\right]; \theta_p = \arcsin(u/l_2) \quad (3.1)$$

The spring length in Fig. 3.1. at the deformed configuration is given by:

$$l_s = \sqrt{\left(l_p + l_1 - l_1 \sqrt{1 - (u/l_2)^2}\right)^2 + u^2 (1 + l_1/l_2)^2} \quad (3.2)$$

Where l_p is the length of the spring when the NSD is un-deformed ($u=0$). The force F_s is the force of the pre-compressed spring given by $F_s = P_{in} - K_s(l_s - l_p)$. Where P_{in} is the pre-compression force of the vertical spring and should have a positive value and K_s is the stiffness of the pre-compressed vertical spring. The total NSD force is: $F_{NSD} = -F_C + F_g - F_s \cos \theta_s (u/h)$. Where h is the height of the double-hinged column, shown in Fig. 2.2.(a), F_g is the force of the gap spring assembly given by Eqn. 3.8. later in this paper and F_C (see Fig. 4) is the horizontal force at point C. F_{NSD} is the external force that needs to be applied on top of the NSD to stabilize it or equivalently the force generated by the NSD and transferred to its top support (structure). Writing the equilibrium equations for the pivot plate using the forces shown in Fig. 3.1. and using Eqn. 3.1.,3.2., one can calculate the horizontal force at point C. The final expression for the NSD force is:

$$F_{NSD} = -\left(\frac{P_{in} + K_s l_p}{l_s} - K_s\right) \left(\frac{l_1}{l_2}\right) \left(2 + \frac{l_p + l_1}{\sqrt{l_2^2 - u^2}} + \frac{l_2}{l_1} \frac{h + l_p + l_1 - (l_1/l_2) \sqrt{l_2^2 - u^2}}{h}\right) u + F_g \quad (3.3)$$

The vertical forces in the NSD caused by the spring's vertical force component create compression on the double hinged columns. When these rotate the horizontal component of their axial load contributes to the total force displacement of the NSD. This is reflected in the third term of Eqn. 3.3., which was derived assuming that the inclination angle of the double hinged columns is small. The height h of the double hinged column is treated as an independent quantity however for most practical implementations it can be assumed that $h \approx l_p + l_1 + l_2$ and therefore Eqn. 3.3. can be further simplified. Note that the effect of the last term in Eqn. 3.3. becomes more and more apparent as the NSD height reduces or as the ratio l_1/l_2 reduces. If these effects can be neglected, then the NSD force can be given by:

$$F_{NSD} = -\left(\frac{P_{in} + K_s l_p}{l_s} - K_s\right) \left(\frac{l_1}{l_2}\right) \left(2 + \frac{l_2}{l_1} + \frac{l_p + l_1}{\sqrt{l_2^2 - u^2}}\right) u + F_g \quad (3.4)$$

The principle of operation of the gap spring assembly is shown in Fig. 3.1.(b). Spring S2 with stiffness k_{s2} of the GSA is pre-compressed by an initial force, P_{is2} (positive) and held in place by a rod and two housing plates. Spring S1 is initially unstressed and its stiffness is k_{s1} . Force F_g is the external force applied to the gap spring assembly, u is the total displacement of the assembly equal to the displacement of housing plate 2, u_h is the total displacement of housing plate 1, d_{gap} is the opening of the gap between housing plate 1 and the reaction plate of spring S1 (the value of d_{gap} should be large enough so that it does not close during the operation of the assembly). F_{s1} is the total force of spring S1, F_{s2} is the total force of spring S2, F_r is the force in the rod connecting the housing plates 1 and 2 and k_r is the stiffness of the rod. k_r is orders of magnitude larger than the stiffness of springs S1 and S2

and its exact value does not affect the GSA force. Also, the stiffness of spring $S1$, is much larger than the stiffness of spring $S2$, typically 20-100 times larger. Once installed, $S2$ is held in place by the nuts of the rod that is passing through the housing plates. Under the action of preload, the rod deforms and the spring slightly reduces its pre-load. Although the loss in preload is very small and the preload value is still P_{is2} , the initial rod deformation given by $u_{in}=P_{is2}/k_r$ is important in the behavior of the assembly. From the free body diagrams of Fig. 3.1.(b), the spring and rod forces can be expressed as; $F_{s1} = k_{s1}u_h$; $F_{s2} = P_{is2} + k_{s2}(u - u_h)$ and

$$F_r = \begin{cases} k_r (P_{is2}/k_r - u + u_h), & u \leq P_{is2}/k_r + u_h \\ 0 & u > P_{is2}/k_r + u_h \end{cases} \quad (3.5)$$

The two parts of Eqn. 3.5. correspond to two stages of operation of the gap spring assembly. The first stage is defined when the force of the rod is nonzero and therefore the rod and nuts are still in contact with spring $S2$. The second stage initiates when the nuts separate from housing plates 1 and 2 and the force of the rod becomes zero. From the free body diagrams of Fig. 3.1.(b), equilibrium of housing plates 1 and 2 requires that: $F_g + F_r - F_{s2} = 0$ and $F_{s1} + F_r - F_{s2} = 0$. Solution of these two equations results in the force-displacement relation of the gap spring assembly for the first stage:

$$u = \left(1 + \frac{k_{s1}}{k_r + k_{s2}}\right) u_h \approx u_h; \quad F_g = \frac{k_{s1}(k_r + k_{s2})}{k_r + k_{s2} + k_{s1}} u \approx k_{s1}u \quad (3.6)$$

Eqn. 3.6. shows that the total displacement of the assembly is approximately equal to the deformation of spring $S1$ and therefore $S2$ moves as a rigid body. This is also reflected in Eqn. 3.6., where the stiffness of the assembly depends almost entirely on the stiffness of spring $S1$. The second stage of operation of the GSA (as shown in Fig. 3.1.(b)(c)) initiates when the rod separates from the housing plates. The displacement and force at which this occurs can be calculated by setting $F_r = 0$ and $u = u'_y$. The result will be:

$$F_g^{u=u'_y} = \left(1 + \frac{k_{s2}}{k_r}\right) P_{is2} \approx P_{is2}; \quad u'_y = \frac{P_{is2}}{k_{s1}} \left(1 + \frac{k_{s1}}{k_r} + \frac{k_{s2}}{k_r}\right) \approx \frac{P_{is2}}{k_{s1}} \quad (3.7)$$

Solution of $F_g + F_r - F_{s2} = 0$ and $F_{s1} + F_r - F_{s2} = 0$, using $F_r = 0$, results in the force-displacement relation of the gap spring assembly during the second stage ($u > u'_y$). Therefore, the complete force displacement of the GSA for a positive displacement is given by:

$$F_g = \begin{cases} k_{s1}u, & 0 \leq u \leq u'_y \\ k_{s1}u'_y + \frac{k_{s2}k_{s1}}{k_{s2} + k_{s1}}(u - u'_y) & u > u'_y \end{cases}; \quad u'_y = \frac{P_{is2}}{k_{s1}} \quad (3.8)$$

Eqn. 3.8. represents a bi-linear elastic force-displacement relation for the GSA which softens when the apparent yield displacement u'_y is reached (see Fig 2.3.). The stiffness of spring $S1$ is selected to be equal to the negative stiffness generated by the NSD at zero displacement, which is equal to

$$k_{s1} = -\frac{P_{in}}{l_p} \frac{l_1}{l_2} \left(2 + \frac{l_p + l_1}{l_2} + \frac{l_2}{l_1} \frac{h + l_p}{h}\right) \quad (3.9)$$

The force versus displacement from Eqn. 3.8. and Eqn. 3.3. for $F_g=0$ are illustrated in Fig. 3.2. for the geometry of the tested device. The force versus displacement relation of the complete device (NSD

plus GSA) using Eqn. 3.3. is shown in Fig. 3.2.(a). Table 3.1. presents the parameters and their magnitude for the device used in the calculations of force in Fig. 3.2.(a). An important property of the NSD is the magnification of stiffness. Eqn. 3.3. reveals the two mechanisms by which this magnification is achieved: (a) the lever ratio l_1/l_2 and (b) another factor that results from the use of the double inverted chevron brace system and the way the components of the device connect to the braces. In order to better understand the significance of stiffness magnification in the NSD, consider a simplified negative stiffness device that only consists of a pre-compressed spring without the magnification mechanisms and the GSA, as shown in Fig. 3.2.(b). This basically is the original idea for the vibration isolation systems of Molyneaux (1957) with the addition of the system being self contained. Once the top of the system in Fig. 3.2.(b) displaces by u , the spring exerts a horizontal force component in the direction of displacement, thus generating negative stiffness. If the height loss due to the pendulum motion of the self containment assembly is neglected, the force displacement of this system is given by:

$$F = - \left(\frac{P_{in} + K_s l_p}{\sqrt{l_p^2 + u^2}} - K_s \right) \left(\frac{h - l_p}{h} \right) u \quad (3.10)$$

A comparison of the force-displacement relation generated by Eqn. 3.10. and Fig 3.3. is shown in Fig. 3.3.(a) and Fig. 3.3.(b). The force is normalized by the spring preload, the length of the spring in the un-deformed position l_p varies in the range 12.7 to 76.4cm and other parameters for the NSD with magnification are as in Table 3.1. The efficiency of the NSD with magnification is apparent. To better illustrate the magnification, the stiffness magnification factor (SMF) at zero displacement was derived after dividing Eqn. 3.3. using $F_g=0$ by Eqn. 3.10. and then letting $u=0$ as:

$$SMF = \frac{l_1}{l_2} \left(2 + \frac{l_2}{l_1} \frac{h+l_p}{h} + \frac{l_p+l_1}{l_2} \right) \frac{h}{h-l_p} \quad (3.11)$$

Fig. 3.3.(c) presents values of the stiffness magnification factor for various values of the lever ratio (l_1/l_2) by varying the value of length l_1 while all other parameters are as presented in Table 3.1. Fig. 3.3.(c) illustrates significant magnification even when the lever ratio is less than unity. Also, the SMF increases with increasing spring length. Note that the tested device has $l_1/l_2=2$ resulting in a value of SMF at zero displacement equal to 48. This significant magnification has a desired major consequence: a proportional reduction in the requirement for spring preload. The tested prototype of NSD had a provision for adjustment of length l_2 so that the magnification factor could be modified by approximately $\pm 3cm$. Fig. 3.3.(d) shows the ranges of behavior that can be achieved by the prototype NSD by modifying the lever ratio in this range.

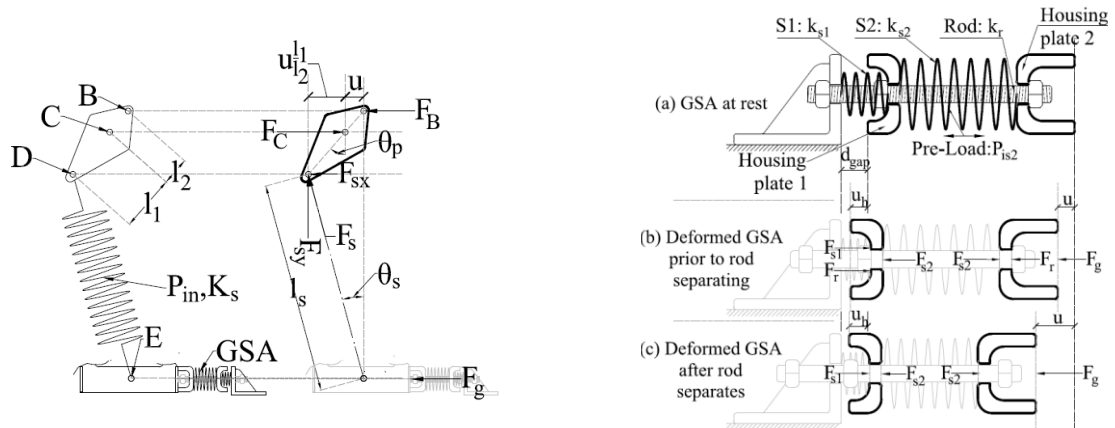


Figure 3.1. (a) Free body diagrams of NSD Center Mechanism; (b) Free body diagram of Gap Spring Assembly

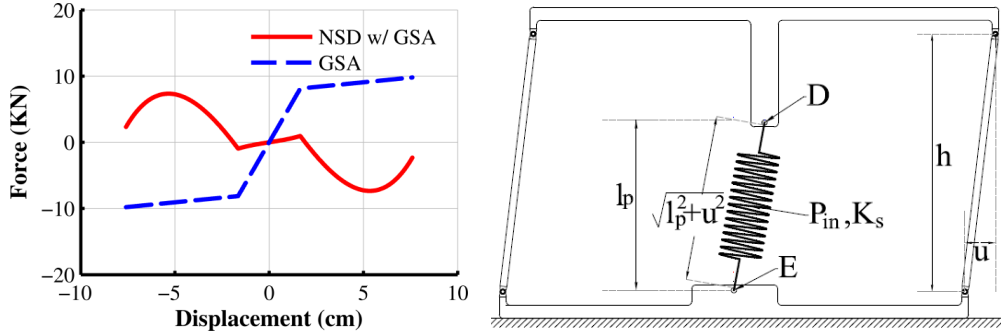


Figure 3.2. (a) Analytical Force-Displacement Relations of Negative Stiffness Device; (b) Simple Negative Stiffness Device without Magnification

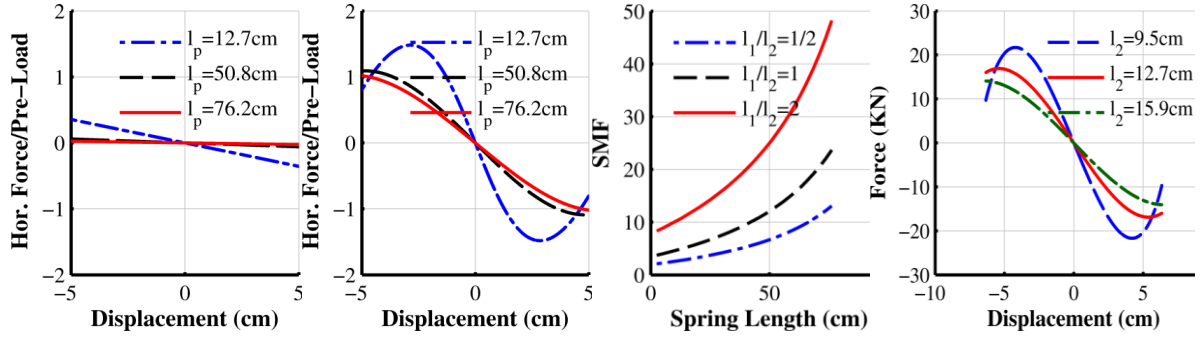


Figure 3.3. Comparison of Normalized Force-displacement Relation of Negative Stiffness Devices [(a): Device without magnification; (b): Device with magnification; (c): Stiffness magnification factor; (d): function of l_2]

4. ANALYTICAL MODEL FOR LARGE ROTATIONS

The formulation in the previous section did not consider large rotations of the lever AB and reduction in the height of the device. These effects become important when the height h of the device and the lever length l_v (see Fig. 2.2.(a) for definition) are comparable in magnitude to the imposed displacement. Fig. 4.1.(a) shows the NSD in its deformed shape. The horizontal lever bar AB is shown rotated and the displacements of points A and B are no longer equal. That is $u = u_A = u_E \neq u_B = -u_D l_2 / l_1$. In order to derive the relation between the displacements of points A and B, consider a reference coordinate system centered at point C in Fig. 4.1.(a). Point B then moves around two circles. One is denoted as $R1$ and is centered at C with a radius l_2 and the other denoted as $R2$ is centered at A at a horizontal distance of $l_v + u$ and vertical distance $l_2 - \Delta h$ from C with a radius l_v . The displacement of point B as a function of the NSD displacement is simply the intersection of the two circles for points located above C ($y > 0$). Once the displacement of point B is expressed as a function of u , the NSD force is calculated by the same process used for the small rotation case:

$$F_{NSD}^{LR} = -F_s \left[\frac{\cos \theta_s (u_B l_1 / l_2 + u \tan \theta) + \sin \theta_s l_1 \sqrt{1 - (u_B / l_2)^2}}{\cos \theta_v \sqrt{l_2^2 - u_B^2} - u_B \sin \theta_v} + \sin \theta_s \right] + F_g \quad (4.1)$$

$$l_s = \sqrt{\left(l_p + l_1 - l_1 \sqrt{1 - (u_B / l_2)^2} + \Delta h \right)^2 + (u + u_B l_1 / l_2)^2} \quad (4.2)$$

$$\theta_s = \arcsin \left[\frac{u / l_s + (u_B l_1) / (l_2 l_s)}{\right]; \quad \theta_v = \arcsin \left[\frac{1}{l_v} \left(l_2 - \sqrt{l_2^2 - u_B^2} - \Delta h \right) \right] \quad (4.3)$$

In Eqn. 4.1. the horizontal component of the double hinged column's axial load has been calculated

$$M_v = \frac{3m_f \bar{y}^2 + m_n h^2}{3(h^2 - u^2)^2} u + \frac{4I_p + m_s l_1^2}{4(l_2^2 - u^2)^2} u - \frac{m_s l_t^2 q}{12r^4 l_s} \left(q \frac{dl_s}{du} + u \cdot l_s \cdot \frac{d^2 l_s}{du^2} \right) + \frac{m_s l_t^4 q^3}{12l_s r^8} u \quad (4.6)$$

$$M_u = K_{NSD}^{eff} - \left(\frac{m_s}{4\sqrt{l_2^2 - u^2}} \frac{l_1}{l_2} + \frac{m_f \bar{y}}{h^2} + \frac{m_h}{2h} \right) g; \quad q = l_s - u \frac{dl_s}{du}; \quad r^4 = l_2^2 l_s^2 - l_t^2 u^2; \quad l_t = l_1 + l_2 \quad (4.7)$$

For the final expressions presented in Eqn. 4.4.-4.7., the spring length l_s and its derivatives with respect to displacement $dl_s/du, d^2l_s/du^2$ can be calculated using Eqn. 3.2., Eqn. 4.1.-4.7. were solved for specified harmonic displacement of $64mm$ amplitude and frequencies in the range of 0 (quasi-static) to $3Hz$ and for the device parameters in Table 3.1. Fig. 4.3.(a) shows the force-displacement relations obtained for the device without and with the GSA. Evidently, there is some limited effect of inertia forces on the calculated force-displacement relations (the larger the frequency, the larger the inertia forces are) but the effects are small for practical purposes. Note that frequencies below $1.5 Hz$ represent the range of fundamental frequency of structures to which such devices may be installed. Finally, Fig. 4.3.(b,c) presents experimental force-displacement relations obtained for the tested prototype of NSD (see also Sarlis, 2012b) in harmonic motion of frequency of $0.1Hz$ and amplitude of $64mm$. The experimental relations are in very good agreement with the analytical relations shown in Fig. 3.2. but for some small hysteresis in the experimental loops. The hysteresis is caused by friction in the joints of the prototype NSD which has not been considered in the analytical models developed in this paper.

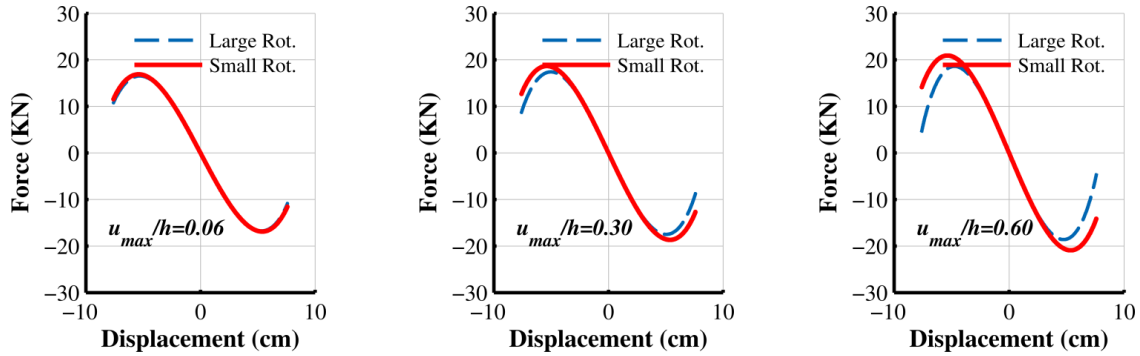


Figure 4.2. Effect of height variation in NSD Force-displacement Relations including Large Rotation Effects

Table 1. Prototype Negative Stiffness Device Properties

Distance	Symbol	Val.	Units	Quantity	Symbol	Value	Units
spring pin to fixed pin	l_1	25.4	cm	Preload	P_{in}	16.5	kN
lever pin to fixed pin	l_2	12.7	cm	Spring S1 –Stiffness	k_{s1}	4.9	kN/cm
Spring length	l_p	76.2	cm	Spring S2 –Stiffness	k_{s2}	0.3	kN/cm
Lever length	l_{lv}	67.3	cm	Spring S2 – Pre-load	P_{is2}	8.1	kN
Double hinged col. height	h	124.5	cm	Spring rate	k_s	1.4	kN/cm
NSD engagement disp.	d_{gap}	1.65	cm				

5. CONCLUSIONS

A Negative Stiffness Device (NSD) was developed and evaluated analytically and experimentally. A detailed description of the operation, component function and design of the device has been presented. It has been shown that a key feature of the device is a large magnification factor for the negative stiffness that substantially reduces the requirements for preload in order to achieve the needed negative stiffness. This feature alone renders the device implementable to structures of large weight. Analytical models of increasing complexity have been developed starting from the simplest possible assuming small rotations to increasing complexity that included large rotation and inertia force effects. It has

been determined that the simplest model without large rotation and inertia force effects is sufficiently accurate for most practical cases.

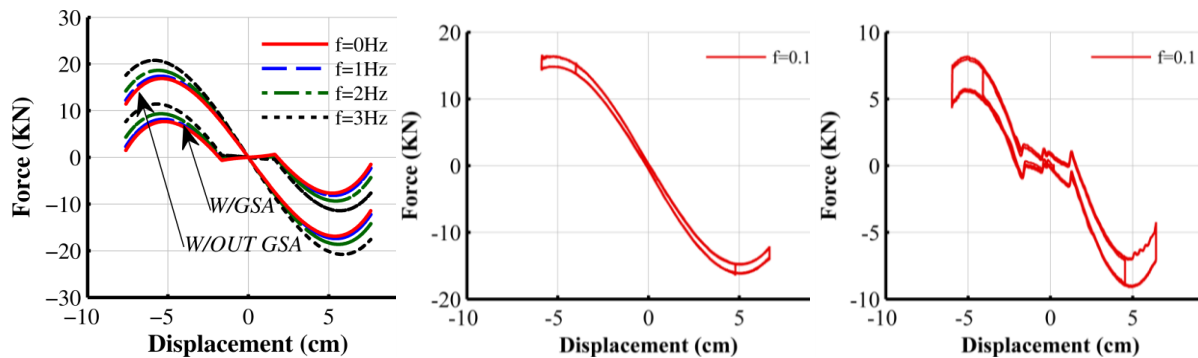


Figure 4.3. (a) Force-displacement Relations of NSD Obtained with Consideration of Inertia Effects; Experimental Force-displacements Relations of NSD [(b): Without GSA; (c): With GSA]

ACKNOWLEDGEMENTS

Funding by National Science Foundation, grant NSF-CMMI--NEESR-0830391 for this project with Dr. Joy Pauschke as program director is gratefully acknowledged. Contributions of David Lee in the development of NSD are gratefully acknowledged.

REFERENCES

- American Society of Civil Engineers (2010), "Minimum design Loads for Buildings and Other Structures", *Standard ASCE 7-10*, Reston, VA.
- Fenz, D.M. and Constantinou, M.C. (2008), "Mechanical Behavior of Multi-spherical Sliding Bearings", *Report No. MCEER-08-0007, Multidisciplinary Center for Earthquake Engineering Research*, Buffalo, NY
- Iemura H. and Pradono M.H. (2009), "Advances in the development of pseudo-negative-stiffness dampers for seismic response control," *Structural Control and Health Monitoring*, **16(7-8)**, 784-799.
- Lee C. M., Goverdovskiy V. and Temnikov A. (2007), "Design of springs with 'negative' stiffness to improve vehicle driver vibration isolation", *Journal of Sound and Vibration* **302(4-5)** 865-874.
- Molyneux W. G. (1957), "Supports for vibration isolation", *ARC/CP-322, Aeronautical Research Council*, Great Britain.
- Nagarajaiah S., Reinhorn A. M., Constantinou M. C., Taylor D., Pasala, D. T. R. and Sarlis, A. A. (2010), "True Adaptive Negative Stiffness: A New Structural Modification Approach for Seismic Protection". *5th World Conference on Structural Control and Monitoring*, Tokyo, Japan, July 12-14
- Pasala, D.T.R, Sarlis A.A., Nagarajaiah S. Reinhorn A.M, Constantinou M.C, and Taylor D., (2012), "Adaptive Negative Stiffness: A New Structural Modification Approach for Seismic Protection", *ASCE / Journal of Structural Engineering* (accepted in March 2012)
- Pavlou, E. and Constantinou, M.C., (2006), "Response of Nonstructural Components in Structures with Damping Systems," *Journal of Structural Engineering, ASCE*, **132(7)**, 1108-1117.
- Platus D.L. (2004), "Vibration Isolation System", US Patent No. 6676101B2, Washington DC: US Patent and Trademark Office.
- Ramirez, O.M., Constantinou, M.C., Kircher, C.A., Whittaker, A.S., Johnson, M.W., Gomez, J.D., and C.Z. Chrysostomou, (2001), "Development and Evaluation of Simplified Procedures for Analysis and Design of Buildings with Passive Energy Dissipation Systems", *Report No. MCEER-00-0010, Revision 1, Multidisciplinary Center for Earthquake Engineering Research*, Buffalo, NY
- Reinhorn A.M., Viti S., and Cimellaro G.P. (2005), "Retrofit of Structures: Strength Reduction with Damping Enhancement", *Proceeding of the 37th UJNR Panel Meeting on Wind and Seismic Effects*, Tsukuba, Japan.
- Roussis, P. C. and Constantinou, M. C., "Uplift-Restraining Friction Pendulum Seismic Isolation System," *Earthquake Engineering and Structural Dynamics*, **35(5)**, 2006, 577-593.
- Sarlis A.A. (2012a), "Adaptive Seismic Protective Systems." Ph.D. Thesis, University at Buffalo, The State University of New York, Buffalo, NY.
- Sarlis A.A., Pasala, D.T.R, Constantinou M.C, Reinhorn A.M, Nagarajaiah S. and Taylor D., (2012b), "Negative Stiffness Device for Seismic Protection of Structures", *ASCE / Journal of Structural Engineering* (accepted in March 2012)
- Viti S., Cimellaro G. P., and Reinhorn A. M. (2006), Retrofit of a Hospital through Strength Reduction and Enhanced Damping. *Smart Structures and Systems*, **2(4)**, 339-355.